UV Irradiation Increases Appetite and Prevents Body Weight Gain through the Upregulation of Norepinephrine in Mice

Qing-Ling Quan[1,2,3,5], Eun Ju Kim[1,2,3,5], Sungsoo Kim[1,2,3], Yeon Kyung Kim[1,2,3], Min Hwa Chung[1,2,3], Yu-Dan Tian[1,2,3], Chang-Yup Shin[1,2,3], Dong Hun Lee[1,2,3] and Jin Ho Chung[1,2,3,4]

UV irradiation of the human skin downregulates lipid synthesis and adipokine production in subcutaneous fat. Recent evidence has suggested that UV exposure limits body weight gain in mouse models of obesity. However, the relationship between norepinephrine and UV irradiation has not been previously reported. Chronic UV exposure stimulated food intake but prevented body weight gain. Leptin, an appetite-suppressing hormone, was significantly reduced in the serum of the UV-irradiated mice. In contrast, UV irradiation induced browning of subcutaneous white adipose tissues without increasing physical activity. Notably, UV irradiation significantly increased norepinephrine levels, and the inhibition of norepinephrine production reversed the effects of chronic UV irradiation on food intake and body weight gain. In conclusion, chronic UV irradiation induces norepinephrine release, resulting in the stimulation of food intake due to the downregulation of leptin levels, but it prevents weight gain by inducing the browning process and elevating energy expenditure.

Keywords: Browning, Leptin, Norepinephrine, Obesity, UV

Journal of Investigative Dermatology (2024) ■, ■–■; doi:10.1016/j.jid.2024.03.012

INTRODUCTION

UVR is a common environmental factor that has multifaceted effects on the skin, which encompasses a substantial surface area of the body. UVR induces detrimental effects such as sunburn, photoaging, and skin cancer; however, it is also associated with beneficial effects such as vitamin D synthesis. We previously showed that UV exposure modulates subcutaneous (SC) fat metabolism in human skin in vivo (Kim et al, 2011). Although UVR cannot directly reach SC fat, it inhibits lipid synthesis and the production of adipokines (adiponectin and leptin) in SC fat through cytokine production in the epidermis and dermis (Kim et al, 2016, 2011). SC fat is now recognized as a pivotal player in metabolic homeostasis (Chait and den Hartigh, 2020), and changes in SC fat may affect energy homeostasis throughout the body. Energy homeostasis maintains a stable internal state between energy intake and expenditure (Hall et al, 2022) and is affected by dietary factors, exercise, and weight changes (Chapelot and Charlot, 2019). UV irradiation prevented metabolic dysfunction and body weight gain in mice fed with a high-fat diet (Ferguson et al, 2019; Fleury et al, 2017; Geldenhuys et al, 2014). However, the mechanism by which UV irradiation modulates energy homeostasis throughout the body has not been fully elucidated. White adipose tissue (WAT) is the primary lipid storage space in adipose tissues. White adipocytes are specialized in storing chemical energy in large triglyceride-enriched lipid droplets with few mitochondria (Seale and Lazar, 2009; Sponton and Kajimura, 2018). In contrast, brown adipose tissue increases energy expenditure and produces heat (Kim and Plutzky, 2016). Brown adipocytes have multiple small lipid droplets and many mitochondria that contain UCP1, which transforms chemical energy into heat (Seale and Lazar, 2009; Sponton and Kajimura, 2018). Increasing the amount of brown adipose tissue or enhancing its function is considered an effective measure for controlling obesity (Kim and Plutzky, 2016). Recently, beige adipocytes have been found to be located in WAT, especially in SC adipose tissues. These are similar to the brown adipose tissue phenotype, with high mitochondrial content, UCP1 expression, and thermogenic capacity upon activation (Kim and Plutzky, 2016). Under proper stimulation, white adipocytes can transform into beige adipocytes, leading to increased thermogenesis in a process known as browning (Bargut et al, 2017). The activation of the browning process may also be an efficient strategy for treating obesity and related metabolic disorders (Kuryłowicz and Puzianowska-Kuźnicka, 2020).

Appetite regulatory pathways are controlled by the CNS and peripheral systems. The CNS is mainly related to the hypothalamus, where neurons in the hypothalamic arcuate nucleus monitor the body's energy state by sensing metabolic

[1]Department of Dermatology, Seoul National University College of Medicine, Seoul, Republic of Korea; [2]Laboratory of Cutaneous Aging Research, Biomedical Research Institute, Seoul National University Hospital, Seoul, Republic of Korea; [3]Institute of Human-Environment Interface Biology, Seoul National University, Seoul, Republic of Korea; and [4]Institute on Aging, Seoul National University, Seoul, Republic of Korea

[5]These authors contributed equally to this work.

Correspondence: Dong Hun Lee, Department of Dermatology, Seoul National University College of Medicine, 101, Daehak-ro, Jongno-gu, Seoul 03080, Republic of Korea. E-mail: ivymed27@snu.ac.kr and Jin Ho Chung, Department of Dermatology, Seoul National University College of Medicine, 101, Daehak-ro, Jongno-gu, Seoul 03080, Republic of Korea. E-mail: jhchung@snu.ac.kr

Abbreviations: AgRP, agouti-related protein; NE, norepinephrine; POMC, pro-opiomelanocortin; SC, subcutaneous; SNS, sympathetic nervous system; WAT, white adipose tissue

Received 12 July 2023; revised 18 February 2024; accepted 4 March 2024; accepted manuscript published online XXX; corrected published online XXX

hormones, including leptin, insulin, and ghrelin, in the systemic circulation (Morton et al, 2014). Activating orexigenic factors such as neuropeptide Y and agouti-related protein (AgRP) induce food intake, whereas activating anorexigenic factors such as pro-opiomelanocortin (POMC) and CART suppress appetite (Chapelot and Charlot, 2019; Seoane-Collazo et al, 2020). In contrast, the peripheral appetite regulatory pathways involve multiple hormone- and nutrient-related signals. Short-term peripheral signals, such as ghrelin, a gastric hormone related to food intake, function as a satiety signal (Morton et al, 2014). However, long-term peripheral signals, such as leptin and insulin, are associated with the status of the energy stores in the body. Leptin, an appetite-suppressing hormone, is primarily produced in WAT and enters the brain through the blood–brain barrier (Zhang and Chua, 2017). Leptin and insulin bind to the arcuate nucleus and regulate central appetite–regulating systems (MacLean et al, 2017).

The sympathetic nervous system (SNS) plays an important role in metabolic homeostasis and in obesity (Larabee et al, 2020). Norepinephrine (NE) is the main neurotransmitter in SNS and functions as a fight-or-flight stress hormone that responds to environmental stressors or dangers (Fitzgerald, 2020). NE is released from sympathetic nerve fibers in adipose tissues under SNS activation, such as a cold challenge, to promote lipolysis and thermogenesis (Larabee et al, 2020). NE is a thermogenesis-related neurotransmitter that binds to β3-adrenergic receptors to produce heat and induce cAMP, which subsequently activates protein kinase A and induces UCP1 in brown fat tissues (Seoane-Collazo et al, 2020). NE prevents weight gain by inducing the browning of WAT (Machado et al, 2022). Meanwhile, NE reduces leptin levels by suppressing leptin mRNA expression through a β3-adrenergic receptor–cAMP–dependent mechanism (Caron et al, 2018). However, the relationship between NE and UV irradiation has not been previously reported.

In this study, we elucidated how chronic UV irradiation of the skin affects energy homeostasis throughout the body.

RESULTS

Chronic UV irradiation promoted food intake but prevented body weight gain

To investigate how chronic UV irradiation influences energy metabolism in the whole body, 4 groups of female C57BL/6 mice were fed normal or high-fat diet and treated with UV or sham irradiation thrice a week for 12 weeks. We conducted 2 parallel studies and quantitatively assessed energy metabolism using Comprehensive Lab Animal Monitoring System cages at baseline and 6 and 12 weeks after UV irradiation (Figure 1a). The food intake and body weight were measured weekly. Normal diet–fed mice exposed to UV irradiation consumed more food than the sham-irradiated mice (Figure 1b). However, despite the increased food intake, the UV-irradiated mice did not gain weight, indicating that UV irradiation could prevent weight gain (Figure 1d). UV-irradiated mice fed with a high-fat diet also showed increased food intake compared with sham-irradiated mice (Figure 1c). UV-irradiated high-fat diet–fed mice had lower body weights than sham-irradiated, high-fat diet–fed mice (Figure 1e). The photographs also demonstrate a consistent pattern of body weight changes in both studies (Figure 1f). The prevention of weight gain in UV-irradiated mice is more marked in the high-fat diet–fed mice than in the normal diet–fed mice. These results indicate that despite increased food intake, UV irradiation could prevent weight gain.

UV exposure modulated orexigenic factors in the hypothalamus through the downregulation of the anorexigenic hormone leptin

Food is the primary source of energy, and overeating impairs energy homeostasis, leading to overweight and obesity (Lee et al, 2020). The hypothalamus plays a key role in controlling food intake by sensing metabolic signals from peripheral organs and modulating feeding behavior (Yu and Kim, 2012). Hypothalamic AgRP and POMC neurons regulate appetite and whole-body energy metabolism in opposing manners (Quarta et al, 2021; Sternson and Atasoy, 2014). To identify how UV irradiation induces increased food intake, we investigated both the central and peripheral appetite regulatory pathways. Among the key regulators of the central appetite pathway, the mRNA levels of neuropeptide Y, an appetite-stimulating factor, were substantially increased in the hypothalamus of UV-irradiated mice fed with a high-fat diet. Both neuropeptide Y and *Agrp* levels tended to increase in UV-irradiated mice fed with a normal diet (Figure 2a). The mRNA expression of appetite-suppressing factors, such as *Pomc* and *Cart*, was not considerably altered in the hypothalamus of UV-irradiated mice (Figure 2b). Immunohistochemistry showed that the protein expression of AgRP was enhanced, and POMC expression was reduced in the arcuate nucleus of the hypothalamus (Figure 2c and d). These data suggest that the UV-induced increase in food intake observed after UV exposure may be associated with an upregulation of orexigenic factors in the hypothalamus.

To explore peripheral appetite regulatory pathways, we examined the serum levels of ghrelin, leptin, and insulin, which can directly regulate appetite through appetite-regulatory neurons in the hypothalamus. Only leptin levels showed a consistent change in both studies (Figure 2e and Supplementary Figure S1a and b). Leptin levels were significantly downregulated as early as week 8 in UV-irradiated mice fed with normal and high-fat diets (Figure 2e). Adipose tissue is the main source of leptin, and fat mass is highly correlated with plasma leptin levels (Chan et al, 2003). Because we previously demonstrated that UVR alters SC fat metabolism in human skin in vivo (Kim et al, 2011), we analyzed the skin and inguinal SC fat tissues. The size of the inguinal SC fat tissue was markedly decreased in high-fat diet–fed mice after chronic UV irradiation (Figure 2f and Supplementary Figure S1c). We found that leptin mRNA expression was significantly decreased in the skin and inguinal SC fat tissues of high-fat diet–fed mice with UV irradiation (Figure 2g and h). Leptin levels tended to be reduced in UV-irradiated mice fed with a normal diet (Figure 2g and h). Leptin plays a pivotal role in energy homeostasis by inhibiting orexigenic neuropeptide Y/AgRP neurons and activating anorexigenic POMC neurons within the hypothalamic arcuate nucleus (Cowley et al, 2001; Jang et al, 2000; Takahashi and Cone, 2005). Our findings

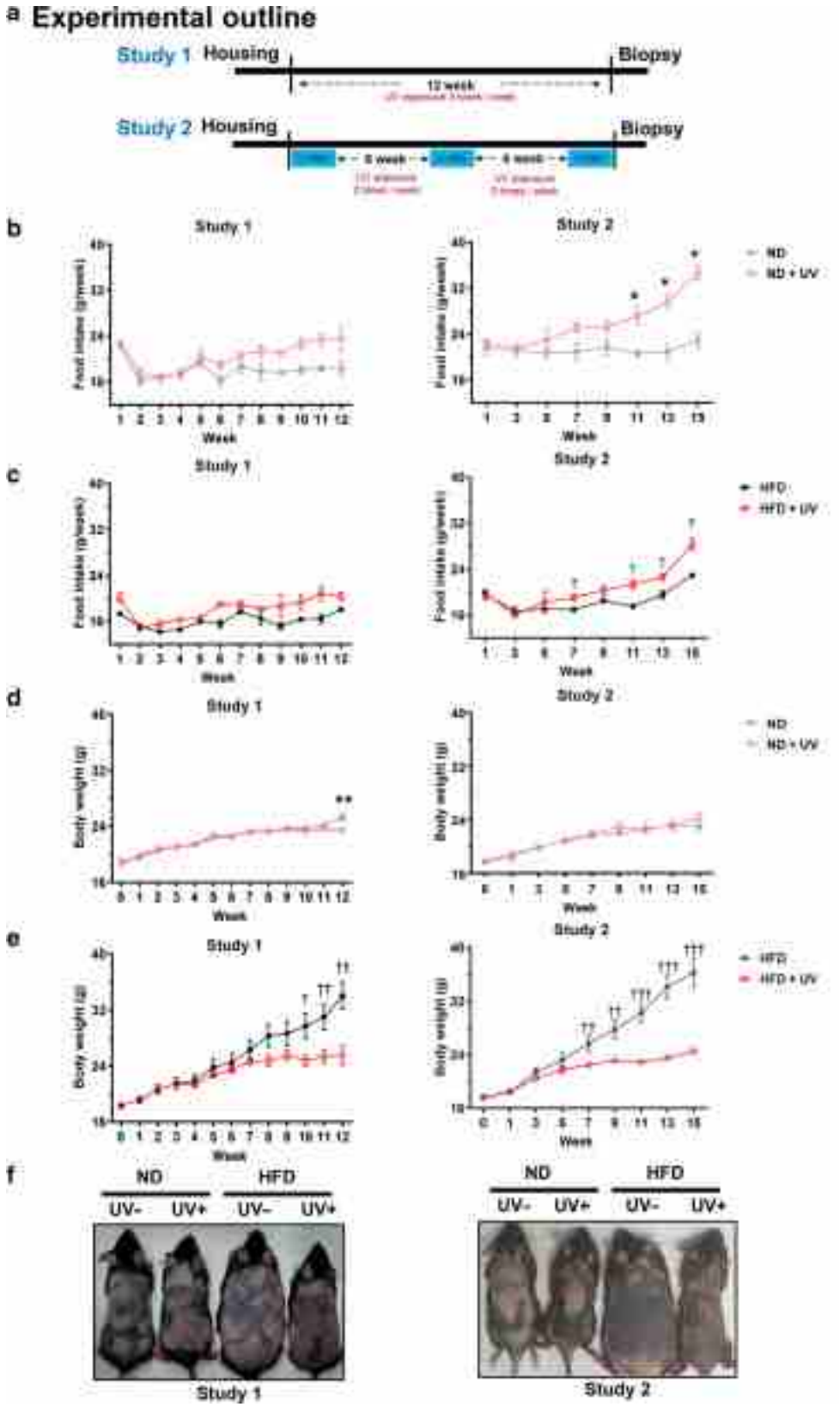

Figure 1. Chronic UV irradiation promotes food intake but prevents body weight gain. HFD- or ND-fed C57BL/6 mice were subjected to UV or sham irradiation for 12 weeks. **(a)** Schematic of the experimental design of studies 1 and 2. In study 2, energy metabolism was quantitatively assessed using CLAMS cages at baseline and after 6 and 12 weeks of UV irradiation. The food intake and body weight of the mice were measured. Cages were periodically used to quantify food intake and body weight changes in study 1 (n = 2 cases per group, 5 mice per case) and study 2 (n = 4 cases per group, 2 mice per case). **(b, c)** Changes in food intake in the ND- and HFD-fed groups. **(d, e)** Changes in body weight in the ND- and HFD-fed groups. **(f)** Comparison of the gross morphology. Representative photographs were obtained after the final UV irradiation. All data are presented as mean ± SEM. $^{*}P < .05$ and $^{**}P < .01$, the sham-irradiated ND-fed group versus the UV-irradiated ND-fed group; $^{\dagger}P < .05$, $^{\dagger\dagger}P < .01$, and $^{\dagger\dagger\dagger}P < .001$, the sham-irradiated HFD-fed group versus the UV-irradiated HFD-fed group. CLAMS, Comprehensive Lab Animal Monitoring System; HFD, high-fat diet; ND, normal diet.

suggest that UV irradiation may reduce leptin synthesis in the skin and inguinal SC fat, which are significant sources of circulating leptin. This reduction could lead to altered serum leptin levels, impacting the regulatory mechanisms of appetite in the hypothalamus and thus promoting an increase in appetite.

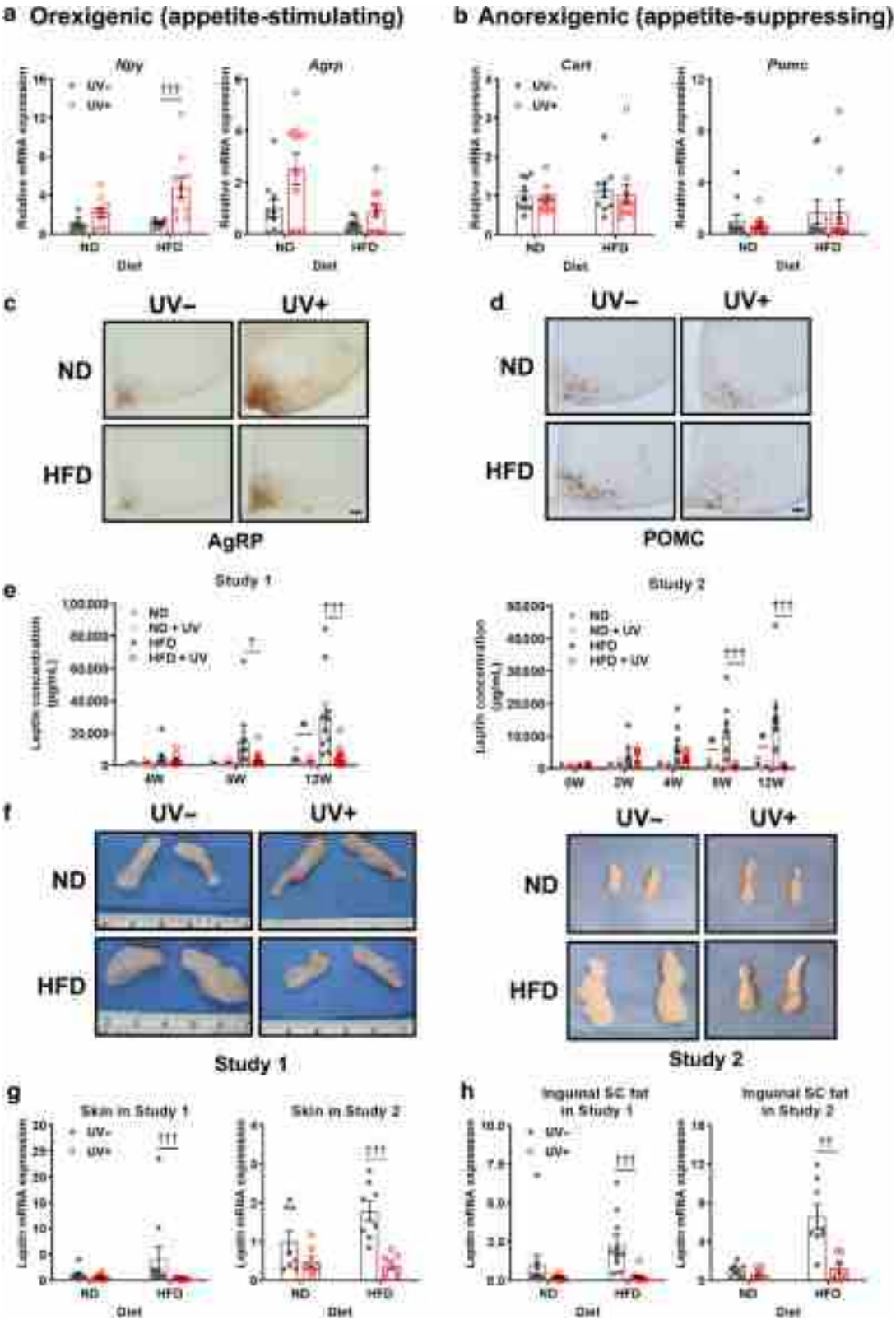

Figure 2. UV exposure modulates orexigenic factors in the hypothalamus and the anorexigenic hormone leptin. Skin, inguinal SC fat, serum, and hypothalamic samples were collected 24 h after UV irradiation after 6 h of fasting. **(a)** Orexigenic factors (*Npy*, *Agrp*) and **(b)** anorexigenic factors (*Pomc* and *Cart*) mRNA levels were analyzed using RT-qPCR in the hypothalamus, and *36b4* was used as an endogenous control (study 1, n = 10 per group). **(c, d)** Immunohistochemical staining was performed to visualize the expression of AgRP and POMC proteins in the mouse hypothalamic arcuate nucleus (study 2, n = 2−3 per group). Bar = 100 μm. **(e)** Changes in serum leptin levels were quantified using an ELISA (study 1, n = 10 per group; study 2, n = 7−8 per group). **(f)** Representative photographs of inguinal SC fat tissues obtained after the last UV-irradiation session. **(g, h)** Leptin mRNA expression levels in the skin and inguinal SC fat tissues were analyzed using RT-qPCR, with *36b4* used as an endogenous control (study 1, n = 10 per group; study 2, n = 7−8 per group). Data are presented as mean ± SEM. $^{*}P < .05$, the sham-irradiated ND-fed group versus the UV-irradiated ND-fed group; $^{\dagger}P < .05$, $^{\dagger\dagger}P < .01$, and $^{\dagger\dagger\dagger}P < .001$, the sham-

UV irradiation induced browning process and UCP1 expression in inguinal SC fat tissues

Chronic UV exposure increased food intake but prevented body weight gain, suggesting that energy expenditure exceeded energy intake. Energy expenditure comprises the resting metabolic rate, physical activity, and thermogenesis (dissipation of energy in the form of heat) (Tran et al, 2022). Inguinal SC fat tissues from the UV-irradiated mice showed a reddish hue (Figure 2f). Histological examination revealed that inguinal SC fat tissues of UV-irradiated mice contained abundant small adipocytes with a multilocular appearance and enhanced eosin staining, which is characteristic of beige adipocytes (Figure 3a). The average adipocyte area significantly decreased in the SC fat tissues of UV-irradiated mice, regardless of the type of diet, indicating that UV irradiation reduced the adipocyte size (Figure 3b). To examine whether UV irradiation induces browning of inguinal WAT, we further investigated changes in thermogenesis-related factors, such as UCP1 and β3-adrenergic receptor. UV irradiation induced substantial increases in UCP1 and β3-adrenergic receptor expression in inguinal SC fat tissues in both the normal and high-fat diet–fed groups (Figure 3c and d). These data indicate that UV irradiation induces browning and thermogenesis-related factors in inguinal SC fat.

UV irradiation induced energy consumption without increasing physical activity

Next, we used Comprehensive Lab Animal Monitoring System cages to evaluate the physical activity associated with UV irradiation. A respiratory exchange ratio of 0.7 indicates that fat is the major fuel source, whereas respiratory exchange ratio of 1 indicates that carbohydrates are the major source. As expected, the respiratory exchange ratio value remained low in mice fed with the high-fat diet (Figure 4a and Supplementary Figure S2a). Chronic UV irradiation significantly increased the oxygen consumption (Figure 4b and Supplementary Figure S2b) and heat generation (Figure 4c and Supplementary Figure S2c), regardless of the light and dark phases. However, chronic UV irradiation did not change physical activity in the normal and high-fat diet–fed groups (Figure 4d). These findings suggest that UV irradiation promotes energy expenditure, which may be due to the browning of SC fat without increased physical activity.

NE synthesis inhibitor, nepicastat, reversed UV-induced changes in food intake and body weight

To identify skin-derived mediators that may cause UV-induced changes in appetite and body weight, we analyzed 28 neurotransmitters in UV-irradiated skin using liquid chromatography/mass spectrometry (Supplementary Table S1). We found that NE levels were significantly increased after chronic UV irradiation. NE levels were significantly increased in the skin and inguinal SC fat tissues after 12 weeks of UV exposure (Figure 5a and b). NE was significantly upregulated in the serum as early as week 2 in UV-irradiated mice (Figure 5c). NE is a well-known thermogenesis-inducing factor and negative modulator of leptin. To determine whether NE is a crucial factor in the effects of UV irradiation on food intake and body weight, high-fat fed mice were treated with UV irradiation and nepicastat (Figure 6a). Nepicastat is an inhibitor of dopamine β-hydroxylase, which catalyzes the conversion of dopamine to NE. After 6 weeks of UV irradiation, the UV-irradiated mice showed increased food intake without body weight gain (Figure 6b and c).

Nepicastat or vehicle was administered from week 7. At week 10, nepicastat significantly mitigated the protective effects of UV irradiation on body weight gain (Figure 6c) and inhibited the UV-induced increase in food intake, albeit not significantly because of the statistical sample size of only 3 (Figure 6b). Moreover, NE levels in the serum, skin, and inguinal SC fat tissues were increased in UV-irradiated mice, and treatment with nepicastat significantly reduced these levels (Figure 6d and e). We also found that leptin levels in the serum (Figure 6f) and skin (Figure 6g) were significantly upregulated in the nepicastat-treated groups compared with those in the vehicle-treated UV-irradiated groups. Leptin levels in inguinal SC fat tissues were also upregulated by nepicastat, but no significant difference was observed (Figure 6g). H&E staining of inguinal SC fat tissues showed that nepicastat reversed the UV-induced decrease in the average adipocyte area of the adipose tissue (Figure 6h and i). Nepicastat also reversed the UV-induced increase in protein levels of UCP1 in the SC fat tissue (Figure 6j and k). Taken together, these results indicate that NE is a critical mediator regulating the metabolic effects of chronic UV irradiation and that nepicastat could reverse the effects of chronic UV irradiation on food intake and body weight by reducing NE levels, upregulating leptin levels, and blocking thermogenesis in SC fat.

DISCUSSION

Appetite is a tightly regulated phenomenon that involves an interplay between various hormones and neurotransmitters to maintain adequate control. These hormones are released from multiple body parts and affect appetite by modulating various factors, including hunger, satiety, and gut mobility (Ans et al, 2018). In this study, we demonstrated that chronic UV irradiation of the skin stimulates food intake by suppressing leptin but prevents weight gain by inducing browning of inguinal SC fat in female mice. Our finding that UV irradiation prevents weight gain in high-fat diet–fed mice is consistent with that of earlier studies, although the appetite response to UV is controversial (Allemann et al, 2020; Ferguson et al, 2019; Geldenhuys et al, 2014).

Allemann et al (2020) showed that low-dose UV exposure (1 kJ/m^2, 2/week) for 12 weeks had no effect on food consumption. Chronic UV exposure (50 mJ/cm^2) for 10 weeks increased food consumption by stimulating ghrelin, which further contributed to weight gain only in male mice and humans (Parikh et al, 2022). Contrary findings showed that UV irradiation prevented weight gain in high-fat–fed mice (Ferguson et al, 2019). Our study revealed that long-term UV exposure increased food intake while preventing weight gain. In our study using female mice, reduced leptin rather than increased ghrelin modulated the UV-induced increase in

irradiated HFD-fed group versus the UV-irradiated HFD-fed group. AgRP, agouti-related protein; CART, cocaine-and-amphetamine-responsive transcript; h, hour; HFD, high-fat diet; ND, normal diet; NPY, neuropeptide Y; POMC, pro-opiomelanocortin; SC, subcutaneous.

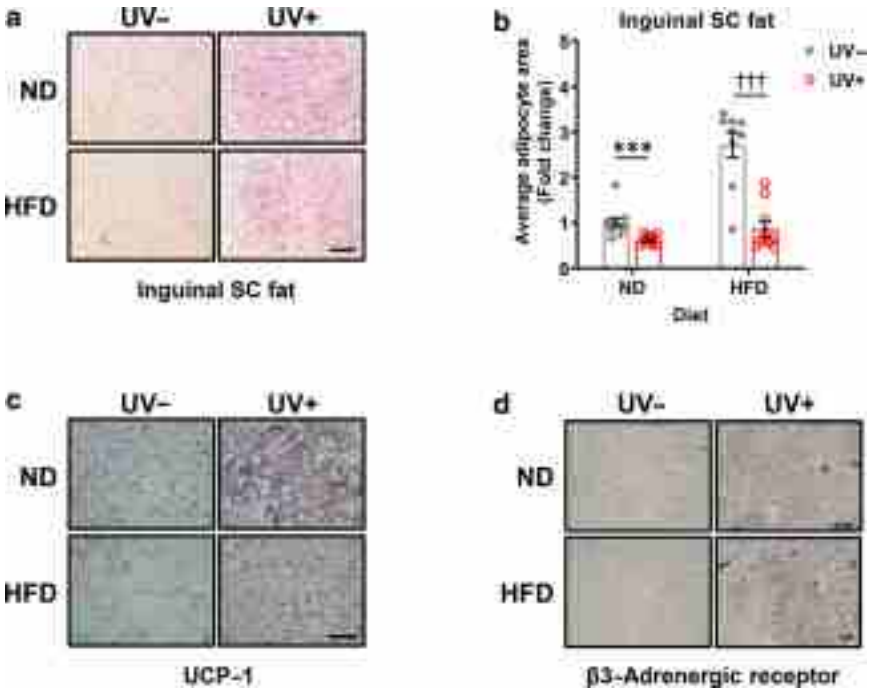

Figure 3. UV irradiation induces browning process and UCP1 expression in inguinal SC fat tissues. **(a)** The inguinal SC fat tissues after 12 weeks of UV irradiation were stained with H&E. **(b)** The average adipocyte area was evaluated using the ImageJ software on the basis of H&E-stained images (n = 9−10 per group). The average area value for each mouse was calculated by measuring the total area of multiple adipocytes in an image, where the cell membrane is intact and contains a region of dissolved empty fat, and then dividing by the number of adipocytes in that region. **(c, d)** Immunohistochemistry showing UCP1 and β3-adrenergic receptor expressions in mouse inguinal SC fat tissues. Bar (for **a**, **c**, and **d**) = 100 μm. Data are presented as fold changes relative to the values of the control group (mean ± SEM). $^{***}P < .001$, the sham-irradiated ND-fed group versus the UV-irradiated ND-fed group; $^{\dagger\dagger\dagger}P < .001$, the sham-irradiated HFD-fed group versus the UV-irradiated HFD-fed group. HFD, high-fat diet; ND, normal diet; SC, subcutaneous.

appetite in mice fed with normal and high-fat diets. Similarly, narrowband UVB phototherapy for psoriasis treatment has been associated with reduced leptin levels (Takahashi et al, 2013). We found no consistent changes in ghrelin levels in the UV-irradiated female mice. Notably, significantly increased food intake in UV-irradiated mice was observed at approximately 7 weeks, when serum leptin levels were considerably reduced. The serum NE levels changed earlier than the serum leptin levels, and the UV-induced reduction in leptin levels was reversed by nepicastat treatment. In addition, UV irradiation suppressed fat accumulation in mice fed with a high-fat diet and decreased leptin mRNA expression in the inguinal SC fat and skin tissues. Treatment with nepicastat also reversed these changes, suggesting that UV irradiation induces appetite by reducing leptin levels through NE release. A loop exists between the white fat tissue and the SNS. Leptin, produced by fat tissue, induces SNS activity, and NE released from SNS nerves not only drives lipolysis and browning (Larabee et al, 2020) but also inhibits leptin synthesis (Caron et al, 2018).

Chronic UV irradiation induced oxygen consumption and heat generation without increasing physical activity, indicating that UV irradiation increases energy expenditure. Energy stored as glucose and fat can be converted into heat in brown and beige adipocytes through UCP1 (Kajimura et al, 2015), leading to browning and beneficial metabolic effects in human WAT (Ans et al, 2018; Herz and Kiefer, 2019). Previous studies have reported that UV irradiation induces UCP1 expression in brown fat tissue, prevents weight gain in high-fat diet–fed mice (Ferguson et al, 2019), and modulates thermogenesis by altering metabolic and immune pathways in interscapular brown adipose tissue (Allemann et al, 2020; Dhamrait et al, 2020). Insulin is recognized as a significant inducer of UCP1 expression (Valverde et al, 2003). However, our data revealed a significant decrease in serum insulin levels after 12 weeks of UV irradiation (Supplementary Figure S1b). This discrepancy suggests that the UV-induced enhancement of UCP1 expression might be independent of insulin modulation. Notably, we found that NE, a major browning activator, was significantly upregulated in UV-irradiated skin. Moreover, the NE synthesis inhibitor, nepicastat, reduced UCP1 expression and increased body weight, showing that NE enhanced energy expenditure by stimulating UCP1 expression and browning in SC fat tissues. Therefore, we propose that NE is a significant modulator of UV-induced changes in energy metabolism.

Although UV irradiation is generally considered beneficial for obesity and metabolic dysfunction (Gorman et al, 2019), the effects of UV irradiation on obesity and metabolic disorders vary considerably in preclinical and clinical studies, depending on the wavelength, dose, animal model (Allemann et al, 2020; Dhamrait et al, 2020; Ferguson et al, 2019; Fleury et al, 2017, 2016; Geldenhuys et al, 2014; Teng et al, 2019), and sex (males or females) (Parikh et al, 2022). Several mediators, such as vitamin D and nitric oxide, have been reported to mediate the effects of UVR (Driver et al, 2008; Fleury et al, 2017; Geldenhuys et al, 2014; Quan et al, 2023; Zhang et al, 2020). In contrast to previous studies, we propose, to our knowledge, a previously unreported NE-dependent mechanism through which UVR

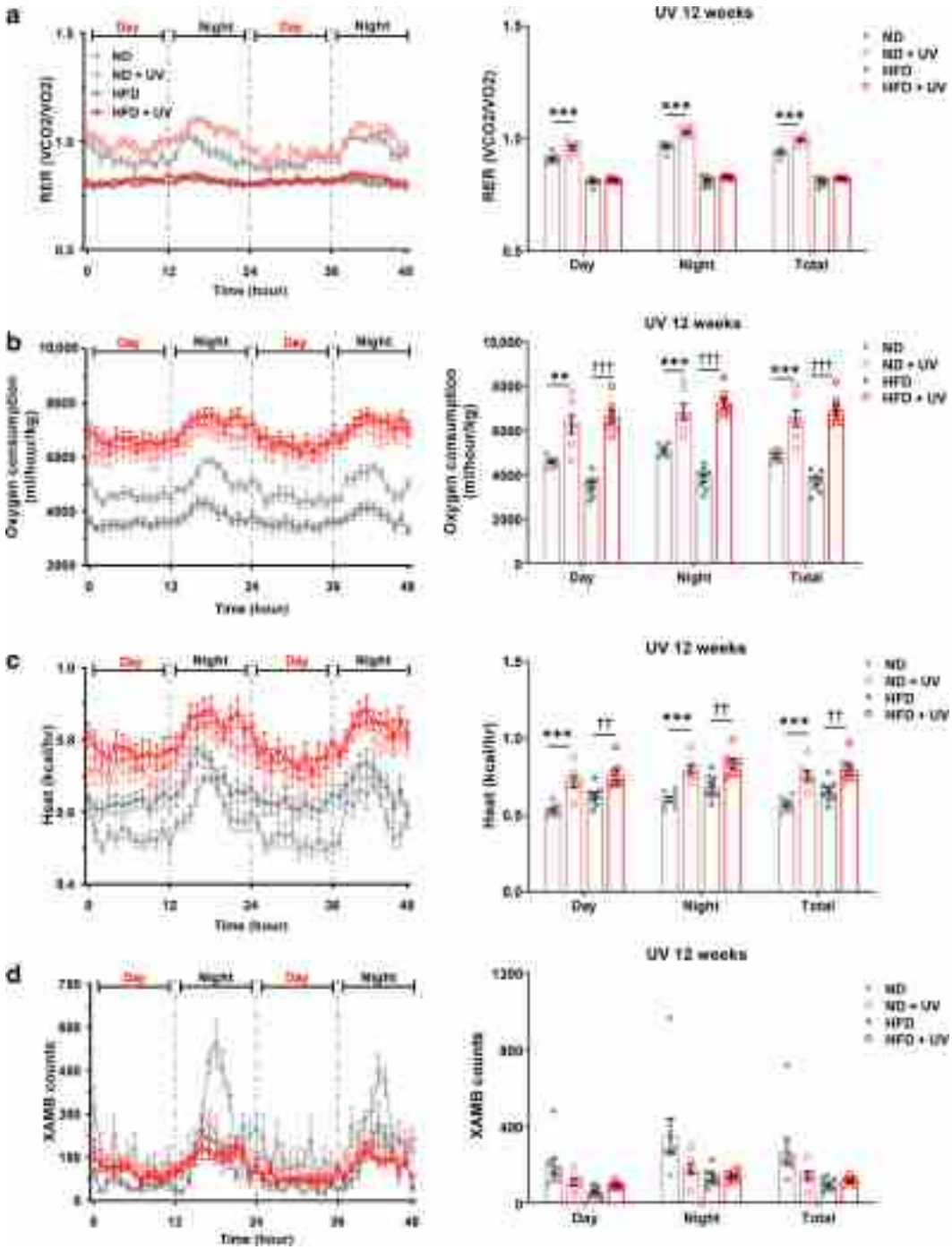

Figure 4. UV irradiation increases energy consumption without increasing physical activity. Mice were individually housed in CLAMS cages for 3 days. After the first 24 h of acclimatization, the RER, oxygen consumption, heat production, and activity were measured. Data for **(a)** RER, **(b)** oxygen consumption, **(c)** heat generation, and **(d)** ambulatory activity counts (denoted as XAMB; walking or running movement on the X-axis) during light and dark cycles after 12 weeks of UV irradiation are shown. Data are presented as mean ± SEM (n = 7–8 per group). $^{**}P < .01$ and $^{***}P < .001$, the sham-irradiated ND-fed group versus the UV-irradiated ND-fed group; $^{\dagger\dagger}P < .01$ and $^{\dagger\dagger\dagger}P < .001$, the sham-irradiated HFD-fed group versus the UV-irradiated HFD-fed group. CLAMS, Comprehensive Lab Animal Monitoring System; h, hour; HFD, high-fat diet; ND, normal diet; RER, respiratory exchange ratio.

regulates the whole-body metabolism. UV-induced NE can mediate body weight control, which is related to many metabolic diseases.

This study has some limitations. We evaluated changes in serum markers at several time points but obtained skin and inguinal SC fat tissues after 12 weeks of chronic UV irradiation; thus, dynamic changes in other tissues might have been missed. However, we validated our results using parallel and independent studies, reinforcing the reliability of our findings. Female mice were selected for this study owing to our observations that male mice exhibit increased aggression after hair removal and UV irradiation, leading to skin wounds and potential inflammatory confounders. Estrogen deficiency has been linked to increased food intake and weight gain (Asarian and Geary, 2002), and this study did not rule out the effect of UV irradiation on estrogen

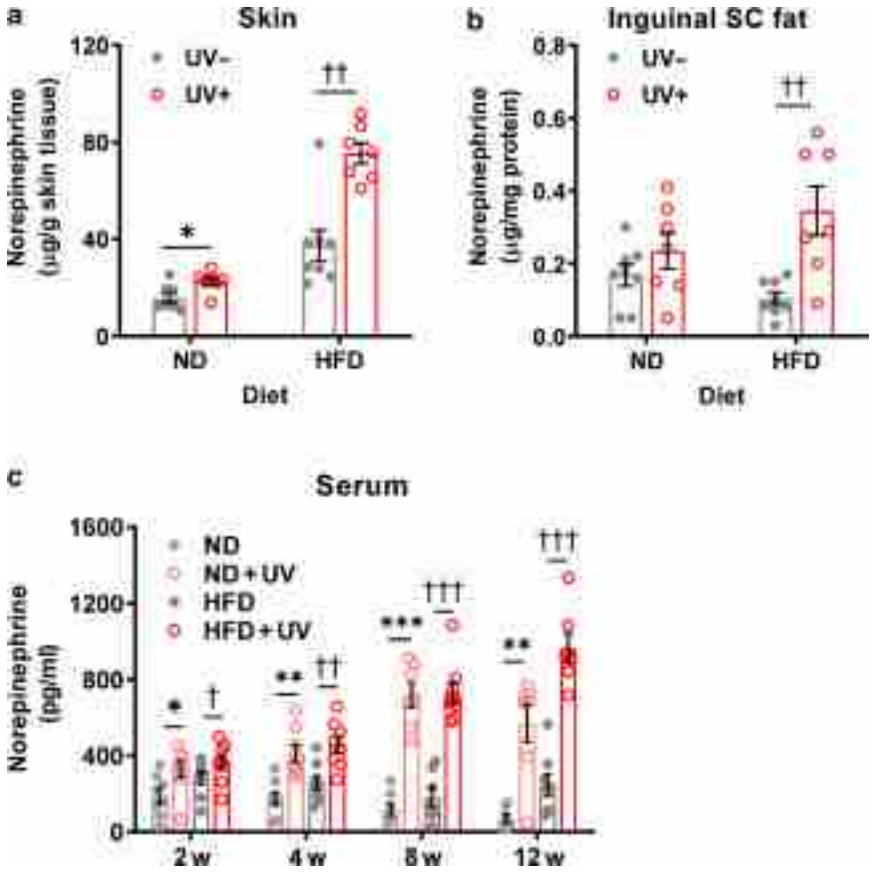

Figure 5. UV irradiation induces norepinephrine release. Skin, inguinal SC fat, and serum samples were collected 24 h after the last UV irradiation at each indicated time point after 6 h of fasting. **(a, b)** Norepinephrine levels in the skin and inguinal SC fat tissues were measured using liquid chromatography–mass spectrometry. **(c)** Serum norepinephrine levels were measured using an ELISA. Data are presented as mean ± SEM (n = 7–8 per group). **P* < .05, ***P* < .01, and ****P* < .001, the sham-irradiated ND-fed group versus the UV-irradiated ND-fed group; †*P* < .05, ††*P* < .01, and †††*P* < .001, the sham-irradiated HFD-fed group versus the UV-irradiated HFD-fed group. h, hour; HFD, high-fat diet; ND, normal diet; SC, subcutaneous.

levels. This warrants further investigation into the specific role of estrogen and its interplay with metabolic changes after chronic UV exposure.

UV irradiation was found to upregulate NE levels in the skin, inguinal SC fat, and serum. Owing to the absence of perfusion prior to sample collection, we cannot entirely rule out the influence of residual blood in the skin and inguinal SC fat on the measured NE levels. Despite this limitation, our in vitro findings provide compelling evidence of the direct effect of UV on NE synthesis. Specifically, UV exposure significantly increased both NE synthesis and dopamine β-hydroxylase mRNA levels in primary human SC adipocytes, whereas no such effects were observed in keratinocytes or fibroblasts (Supplementary Figure S3). Given the established role of adipocytes as a source of catecholamine production (Vargovic et al, 2011), our findings suggest that adipocytes within the skin could significantly contribute to the observed increase in UV-induced NE.

In conclusion, our study provides evidence that chronic UV irradiation of the skin stimulates food intake and modulates body weight through NE by suppressing leptin expression and enhancing the orexigenic pathway in the hypothalamus. UV-induced NE also triggers the browning of inguinal SC fat tissues and prevents the weight gain associated with excess energy intake. These findings suggest that UVR can be used as a potential therapeutic intervention for obesity-associated metabolic disorders.

MATERIALS AND METHODS

Animals and treatment

Female C57BL/6 mice aged 5 weeks were purchased from the Orient Experimental Animal Breeding Center and housed under standard controlled room conditions (22 ± 2 °C temperature and 50 ± 10% humidity) with food and water available ad libitum.

After 1 week of acclimatization, the mice were randomly allocated to 4 groups and fed either a normal diet (10% kcal from fat, 70% kcal from carbohydrates, 20% kcal from protein, D06072701; Research Diets) or high-fat diet (60% kcal from fat, 20% kcal from carbohydrates, 20% kcal from protein, D07012601; Research Diets) with UV or sham irradiation. Food intake and body weight were measured weekly. The dorsal skin was shaved, and the hair was removed weekly. Mice were treated with UV irradiation thrice a week for 12 weeks, as previously described (Kim et al, 2005). F75/85W/UV21 fluorescent sunlamps were utilized as the UV source. These lamps emit wavelengths ranging from 275 to 380 nm, with a peak emission between 310 and 315 nm. UVC radiation (wavelengths <290 nm) was filtered out. The intensity of UV irradiation was measured using a UV meter (Model 585100; Waldmann).

In both study 1 and study 2, the UV irradiation dose was incrementally increased every 2 weeks, starting from 100 mJ/cm^2 (equivalent to 1 minimal erythema/edema dose) and escalating to 400 mJ/cm^2. It was then maintained at 4 minimal erythema doses until the end of the 12-week period, resulting in a total accumulated dose of 10,800 mJ/cm^2. Typically, the mouse skin displayed mild erythema after each UV irradiation session. If the mouse skin showed only mild erythema or no signs of inflammation after UV exposure,

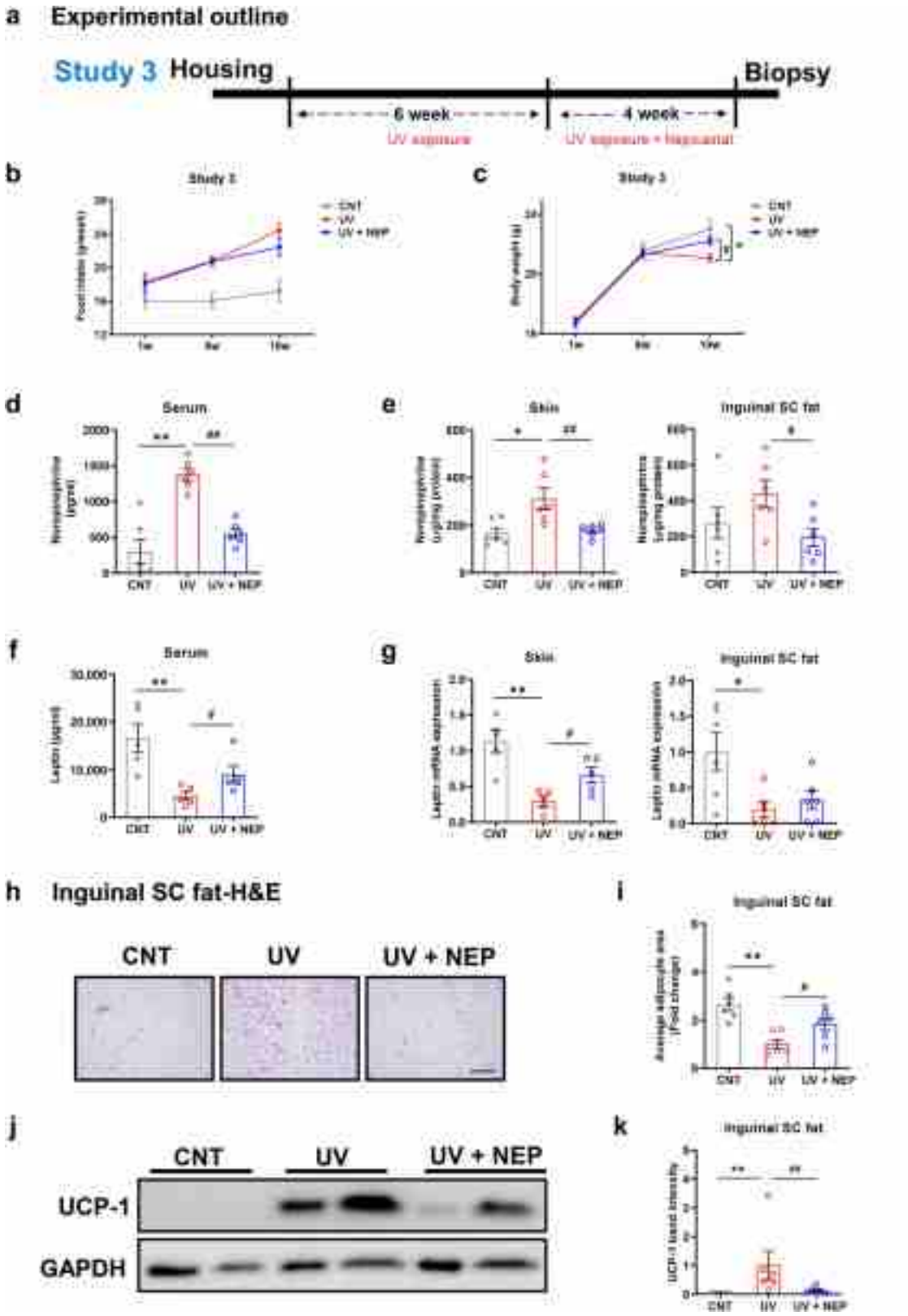

Figure 6. Norepinephrine synthesis inhibitor, NEP, reverses UV-induced changes in food intake and body weight. In study 3, HFD-fed C57BL/6 female mice were subjected to UV or sham irradiation for 10 weeks. The NEP treatment group received an intraperitoneal injection of 30 mg/kg NEP hydrochloride 6 weeks after study initiation. After 10 weeks, skin, inguinal SC fat, and serum samples were obtained. **(a)** Schematic of the experimental design of study 3. **(b, c)** Changes in food intake and body weight (n = 3 cases per group, 2 mice per case). **(d)** Serum norepinephrine levels were measured using an ELISA (n = 6 per group). **(e)** Norepinephrine levels in the inguinal SC fat and skin tissues were measured using liquid chromatography−mass spectrometry (n = 6 per group). **(f)** Serum leptin levels were measured using ELISA (n = 5 per group). **(g)** Leptin mRNA levels in the inguinal SC fat and skin tissues were analyzed using RT-qPCR, with *36b4* used as an endogenous control (n = 5−6 per group). **(h, i)** Inguinal fat tissues were stained with H&E, and the average adipocyte area was quantified

the fluence was incrementally increased. Furthermore, the eyes were covered to exclude the effects of UVR on whole-body metabolism through the eyes rather than the skin.

For the nepicastat experiment, 30 mg/kg nepicastat hydrochloride (SML0940, Sigma-Aldrich) was dissolved in saline containing 1.5% dimethylsulfoxide and 1.5% Cremophor EL (Sigma-Aldrich) (Schroeder et al, 2013) and intraperitoneally injected after 6-week UV irradiation. The mice were irradiated with UV thrice per week for 10 weeks. The UV irradiation dose was gradually increased from 100 to 300 mJ/cm^2, and total amount was 7200 mJ/cm^2 in study 3.

All experimental protocols were approved by the Institutional Animal Care and Use Committee of the Seoul National University Hospital.

Immunohistochemistry

The inguinal fat tissue was fixed in 4% paraformaldehyde and embedded in paraffin blocks. The samples (with 4-μm thickness) were sectioned and stained with H&E. For immunohistochemical staining, after rehydration with ethanol and antigen retrieval with Target Retrieval Solution (Dako), fat tissue sections were blocked with a preblocking solution (GBI Labs). Primary antibodies against UCP1 (ab10983, Abcam) and β3-adrenergic receptor (ab94506, Abcam) were 1:200 diluted in Diluent Buffer (Dako) at 4 °C overnight. The slides were incubated with the secondary antibody from the Splink HRP Broad Bulk kit (GBI Labs) and visualized using 3,3′-diaminobenzidine (Vector Laboratories). Finally, hematoxylin was used to counterstain the nuclei with a blue-violet color. The staining results are presented as images obtained using a light microscope (DM5500B, Leica Microsystems).

Mouse brain was fixed in 4% paraformaldehyde overnight, transferred to a 30% sucrose solution at 4 °C, embedded in Tissue-Tek optimal cutting temperature compound (Sakura Finetech), and stored at −80 °C, as described previously (Han et al, 2017). The samples were sectioned at 40-μm thickness and then treated with antigen retrieval. The POMC and AgRP primary antibody (1:200, Abcam) was incubated at 4 °C overnight, and the secondary antibody was incubated for 1 hour at room temperature. A Vector ABC kit (Vector Laboratories) was used to enhance the signal, and 3,3′-diaminobenzidine (Vector Laboratories) was used for color development. Images were captured and analyzed using a light microscope, as described earlier.

RNA extraction

Skin, inguinal WAT, and hypothalamus samples were extracted with RNA using RNAiso (Takara Bio), and total RNA (1 μg) was converted to cDNA using First Strand cDNA Synthesis Kit (MBI Fermentas), according to the manufacturer's instructions. RT-qPCR was performed using a 7500 Real-time PCR System (Applied Biosystems) with SYBR Premix Ex Taq (Takara Bio), as previously described (Hong et al, 2019). The primers used are listed in Supplementary Table S2.

ELISA

Blood samples were collected in serum separator tubes (BD Microtainer Tubes) 24 hours after UV irradiation and after 6 hours of fasting. After centrifugation at 3500*g* for 20 minutes at 4 °C, serum was obtained and stored at −80 °C. Leptin and NE levels were analyzed using commercially available kits (BioVision), according to the manufacturer's instructions.

Western blotting

Inguinal fat tissue samples were lysed using a radioimmunoprecipitation assay lysis buffer (EMD Millipore) supplemented with protease and phosphatase inhibitors (Thermo Fisher Scientific). After homogenization, the lysate was centrifuged at 15,000*g* for 30 minutes at 4 °C, and the supernatant was recovered. The protein concentration was determined using a BCA Assay Kit (Biomax) and adjusted to 1 mg/ml. The prepared samples were separated and transferred onto membranes. After blocking, the membrane was incubated with primary antibodies against UCP1 (ab10983, Abcam) and GAPDH (Thermo Fisher Scientific) at 4 °C overnight. The blot was developed after incubation with a horseradish peroxidase–conjugated secondary antibody (Gentex) using the Pierce ECL Western Blotting Substrate (Thermo Fisher Scientific). Blots were developed according to the manufacturer's instructions.

Liquid chromatography–mass spectrometry

NE levels in the skin and in inguinal WAT tissues were quantified using liquid chromatography–mass spectrometry, as previously reported (Woo et al, 2018). Skin and inguinal WAT tissues were weighted and homogenized with dilution factors of 200 and 20 μl/mg, respectively. The liquid chromatography–tandem mass spectrometry system comprised the ExionLC system and the 6500+ QTRAP mass spectrometer, equipped with an electrospray ionization source. Data collection and quantification were performed using Analyst software, version 1.7. Chromatographic separation was achieved on a Waters Acquity HSS T3 column (2.1 × 100 mm, 1.8 μm). The column and autosampler tray temperatures were maintained at 50 and 4 °C, respectively. The mobile phases consisted of a 0.1% aqueous formic acid solution (A) and a 5 mM ammonium formate solution in acetonitrile (B). The injection volume was set at 10 μl, with a flow rate of 0.3 ml/min. Both positive and negative ion modes of the mass spectrometer were optimized for multiple reaction monitoring scanning.

Comprehensive Lab Animal Monitoring System

The mice were housed alone within Comprehensive Lab Animal Monitoring System cages (Columbus Instruments) for 3 days at baseline, after 6 weeks, and after 12 weeks of UV irradiation. The oxygen and carbon dioxide concentrations at the entry and exit points were monitored using a calorimetry system. Energy expenditure, the respiratory exchange ratio, oxygen consumption, heat production, and activity were measured after the initial 24 hours of acclimatization. All data were averaged over 2 days.

Statistical analysis

Statistical analyses were performed using the Statistical Package for the Social Sciences (version 22.0; IBM) software. The results are presented as the mean ± SEM. Significant differences between the groups were analyzed using a 2-tailed Mann–Whitney *U* test. $P < .05$ was considered statistically significant.

DATA AVAILABILITY STATEMENT

No large datasets were generated in these studies.

(n = 6 per group). Bar = 100 μm. **(j, k)** UCP1 protein levels in the inguinal fat were assessed using western blotting. GAPDH was used as a loading control. Band densities were analyzed using the ImageJ software (n = 6 per group). Data are presented as mean ± SEM. *$P < .05$ and **$P < .01$, the sham-irradiated control group versus the UV-irradiated group; $^{\#}P < .05$ and $^{\#\#}P < .01$, the UV-irradiated control group versus the UV-irradiated group with NEP. NEP, nepicastat; SC, subcutaneous.

ORCIDs

Qing-Ling Quan: http://orcid.org/0009-0000-7575-6556
Eun Ju Kim: http://orcid.org/0000-0002-6840-2888
Sungsoo Kim: http://orcid.org/0009-0005-8988-327X
Yeon Kyung Kim: http://orcid.org/0000-0002-3080-9818
Min Hwa Chung: http://orcid.org/0009-0000-1288-8199
Yu-Dan Tian: http://orcid.org/0009-0003-4996-8485
Chang-Yup Shin: http://orcid.org/0009-0009-2957-778X
Dong Hun Lee: http://orcid.org/0000-0002-2925-3074
Jin Ho Chung: http://orcid.org/0000-0002-0934-1632

CONFLICT OF INTEREST

The authors state no conflict of interest.

ACKNOWLEDGMENTS

This research was supported by the New Faculty Startup Fund from Seoul National University (grant number 0411-20180042); the Ministry of Health & Welfare, Republic of Korea (grant number HI14C1277); and a grant from the National Research Foundation of Korea funded by the Korean government (2013R1A1A1065100, 2015R1D1A1A01059179, and 2019R1F1A1053234). The guarantor of this study is DHL.

AUTHOR CONTRIBUTIONS

Conceptualization: DHL, JHC; Data Curation: Q-LQ, EJK; Investigation: Q-LQ, EJK, SK, Y-DT, MHC; Methodology: Q-LQ, YKK, C-YS; Writing – Original Draft Preparation: Q-LQ, EJK; Writing - Review and Editing: Q-LQ, EJK, DHL, JHC

SUPPLEMENTARY MATERIAL

Supplementary material is linked to the online version of the paper at www.jidonline.org, and at https://doi.org/10.1016/j.jid.2024.03.012.

REFERENCES

Allemann TS, Dhamrait GK, Fleury NJ, Abel TN, Hart PH, Lucas RM, et al. Low-dose UV radiation before running wheel access activates brown adipose tissue. J Endocrinol 2020;244:473–86.

Ans AH, Anjum I, Satija V, Inayat A, Asghar Z, Akram I, et al. Neurohormonal regulation of appetite and its relationship with stress: a mini literature review. Cureus 2018;10:e3032.

Asarian L, Geary N. Cyclic estradiol treatment normalizes body weight and restores physiological patterns of spontaneous feeding and sexual receptivity in ovariectomized rats. Horm Behav 2002;42:461–71.

Bargut TCL, Souza-Mello V, Aguila MB, Mandarim-de-Lacerda CA. Browning of white adipose tissue: lessons from experimental models. Horm Mol Biol Clin Investig 2017. 31:/j/hmbci.2017.31.

Caron A, Lee S, Elmquist JK, Gautron L. Leptin and brain-adipose crosstalks. Nat Rev Neurosci 2018;19:153–65.

Chait A, den Hartigh LJ. Adipose tissue distribution, inflammation and its metabolic consequences, including diabetes and cardiovascular disease. Front Cardiovasc Med 2020;7:22.

Chan JL, Heist K, DePaoli AM, Veldhuis JD, Mantzoros CS. The role of falling leptin levels in the neuroendocrine and metabolic adaptation to short-term starvation in healthy men. J Clin Invest 2003;111:1409–21.

Chapelot D, Charlot K. Physiology of energy homeostasis: models, actors, challenges and the glucoadipostatic loop. Metabolism 2019;92:11–25.

Cowley MA, Smart JL, Rubinstein M, Cerdán MG, Diano S, Horvath TL, et al. Leptin activates anorexigenic POMC neurons through a neural network in the arcuate nucleus. Nature 2001;411:480–4.

Dhamrait GK, Panchal K, Fleury NJ, Abel TN, Ancliffe MK, Crew RC, et al. Characterising nitric oxide-mediated metabolic benefits of low-dose ultraviolet radiation in the mouse: a focus on brown adipose tissue. Diabetologia 2020;63:179–93.

Driver JP, Foreman O, Mathieu C, van Etten E, Serreze DV. Comparative therapeutic effects of orally administered 1,25-dihydroxyvitamin D(3) and 1alpha-hydroxyvitamin D(3) on type-1 diabetes in non-obese diabetic mice fed a normal-calcaemic diet. Clin Exp Immunol 2008;151:76–85.

Ferguson AL, Kok LF, Luong JK, Van Den Bergh M, Bell-Anderson KS, Fazakerley DJ, et al. Exposure to solar ultraviolet radiation limits diet-induced weight gain, increases liver triglycerides and prevents the early signs of cardiovascular disease in mice. Nutr Metab Cardiovasc Dis 2019;29:633–8.

Fitzgerald PJ. Norepinephrine release may play a critical role in the Warburg effect: an integrative model of tumorigenesis. Neoplasma 2020;67:947–57.

Fleury N, Feelisch M, Hart PH, Weller RB, Smoothy J, Matthews VB, et al. Sub-erythemal ultraviolet radiation reduces metabolic dysfunction in already overweight mice. J Endocrinol 2017;233:81–92.

Fleury N, Geldenhuys S, Gorman S. Sun exposure and its effects on human health: mechanisms through which sun exposure could reduce the risk of developing obesity and cardiometabolic dysfunction. Int J Environ Res Public Health 2016;13:999.

Geldenhuys S, Hart PH, Endersby R, Jacoby P, Feelisch M, Weller RB, et al. Ultraviolet radiation suppresses obesity and symptoms of metabolic syndrome independently of vitamin D in mice fed a high-fat diet. Diabetes 2014;63:3759–69.

Gorman S, de Courten B, Lucas RM. Systematic review of the effects of ultraviolet radiation on markers of metabolic dysfunction. Clin Biochem Rev 2019;40:147–62.

Hall KD, Farooqi IS, Friedman JM, Klein S, Loos RJF, Mangelsdorf DJ, et al. The energy balance model of obesity: beyond calories in, calories out. Am J Clin Nutr 2022;115:1243–54.

Han M, Ban JJ, Bae JS, Shin CY, Lee DH, Chung JH. UV irradiation to mouse skin decreases hippocampal neurogenesis and synaptic protein expression via HPA axis activation. Sci Rep 2017;7:15574.

Herz CT, Kiefer FW. Adipose tissue browning in mice and humans. J Endocrinol 2019;241:R97–109.

Hong JS, Han S, Lee JS, Lee C, Choi MH, Kim YK, et al. Abnormal glucocorticoid synthesis in the lesional skin of erythematotelangiectatic rosacea. J Invest Dermatol 2019;139:2225–8.e3.

Jang M, Mistry A, Swick AG, Romsos DR. Leptin rapidly inhibits hypothalamic neuropeptide Y secretion and stimulates corticotropin-releasing hormone secretion in adrenalectomized mice. J Nutr 2000;130:2813–20.

Kajimura S, Spiegelman BM, Seale P. Brown and beige fat: physiological roles beyond heat generation. Cell Metab 2015;22:546–59.

Kim EJ, Kim YK, Kim JE, Kim S, Kim MK, Park CH, et al. UV modulation of subcutaneous fat metabolism. J Invest Dermatol 2011;131:1720–6.

Kim EJ, Kim YK, Kim MK, Kim S, Kim JY, Lee DH, et al. UV-induced inhibition of adipokine production in subcutaneous fat aggravates dermal matrix degradation in human skin. Sci Rep 2016;6:25616.

Kim HH, Lee MJ, Lee SR, Kim KH, Cho KH, Eun HC, et al. Augmentation of UV-induced skin wrinkling by infrared irradiation in hairless mice. Mech Ageing Dev 2005;126:1170–7.

Kim SH, Plutzky J. Brown fat and browning for the treatment of obesity and related metabolic disorders. Diabetes Metab J 2016;40:12–21.

Kuryłowicz A, Puzianowska-Kuźnicka M. Induction of adipose tissue browning as a strategy to combat obesity. Int J Mol Sci 2020;21:6241.

Larabee CM, Neely OC, Domingos AI. Obesity: a neuroimmunometabolic perspective. Nat Rev Endocrinol 2020;16:30–43.

Lee SY, Kang HJ, Hur SJ. Overview of energy intake, physical activity, and neuronal substances on obesity. Food Life 2020:1–11.

Machado SA, Pasquarelli-do-Nascimento G, da Silva DS, Farias GR, de Oliveira Santos I, Baptista LB, et al. Browning of the white adipose tissue regulation: new insights into nutritional and metabolic relevance in health and diseases. Nutr Metab (Lond) 2022;19:61.

MacLean PS, Blundell JE, Mennella JA, Batterham RL. Biological control of appetite: a daunting complexity. Obesity (Silver Spring) 2017;25:S8–16.

Morton GJ, Meek TH, Schwartz MW. Neurobiology of food intake in health and disease. Nat Rev Neurosci 2014;15:367–78.

Parikh S, Parikh R, Michael K, Bikovski L, Barnabas G, Mardamshina M, et al. Food-seeking behavior is triggered by skin ultraviolet exposure in males. Nat Metab 2022;4:883–900.

Quan QL, Yoon KN, Lee JS, Kim EJ, Lee DH. Impact of ultraviolet radiation on cardiovascular and metabolic disorders: the role of nitric oxide and vitamin D. Photodermatol Photoimmunol Photomed 2023;39:573–81.

Quarta C, Claret M, Zeltser LM, Williams KW, Yeo GSH, Tschöp MH, et al. POMC neuronal heterogeneity in energy balance and beyond: an integrated view. Nat Metab 2021;3:299–308.

Schroeder JP, Epps SA, Grice TW, Weinshenker D. The selective dopamine β-hydroxylase inhibitor nepicastat attenuates multiple aspects of cocaine-seeking behavior. Neuropsychopharmacology 2013;38:1032–8.

Seale P, Lazar MA. Brown fat in humans: turning up the heat on obesity. Diabetes 2009;58:1482–4.

Seoane-Collazo P, Martínez-Sánchez N, Milbank E, Contreras C. Incendiary leptin. Nutrients 2020;12:472.

Sponton CH, Kajimura S. Multifaceted roles of beige fat in energy homeostasis beyond UCP1. Endocrinology 2018;159:2545–53.

Sternson SM, Atasoy D. Agouti-related protein neuron circuits that regulate appetite. Neuroendocrinology 2014;100:95–102.

Takahashi H, Tsuji H, Ishida-Yamamoto A, Iizuka H. Serum level of adiponectin increases and those of leptin and resistin decrease following the treatment of psoriasis. J Dermatol 2013;40:475–6.

Takahashi KA, Cone RD. Fasting induces a large, leptin-dependent increase in the intrinsic action potential frequency of orexigenic arcuate nucleus neuropeptide Y/Agouti-related protein neurons. Endocrinology 2005;146:1043–7.

Teng S, Chakravorty L, Fleury N, Gorman S. Regular exposure to non-burning ultraviolet radiation reduces signs of non-alcoholic fatty liver disease in mature adult mice fed a high fat diet: results of a pilot study. BMC Res Notes 2019;12:78.

Tran LT, Park S, Kim SK, Lee JS, Kim KW, Kwon O. Hypothalamic control of energy expenditure and thermogenesis. Exp Mol Med 2022;54:358–69.

Valverde AM, Arribas M, Mur C, Navarro P, Pons S, Cassard-Doulcier AM, et al. Insulin-induced up-regulated uncoupling protein-1 expression is mediated by insulin receptor substrate 1 through the phosphatidylinositol 3-kinase/Akt signaling pathway in fetal brown adipocytes. J Biol Chem 2003;278:10221–31.

Vargovic P, Ukropec J, Laukova M, Cleary S, Manz B, Pacak K, et al. Adipocytes as a new source of catecholamine production. FEBS Lett 2011;585:2279–84.

Woo J, Min JO, Kang DS, Kim YS, Jung GH, Park HJ, et al. Control of motor coordination by astrocytic tonic GABA release through modulation of excitation/inhibition balance in cerebellum. Proc Natl Acad Sci U S A 2018;115:5004–9.

Yu JH, Kim MS. Molecular mechanisms of appetite regulation. Diabetes Metab J 2012;36:391–8.

Zhang H, Shen Z, Lin Y, Zhang J, Zhang Y, Liu P, et al. Vitamin D receptor targets hepatocyte nuclear factor 4α and mediates protective effects of vitamin D in nonalcoholic fatty liver disease. J Biol Chem 2020;295:3891–905.

Zhang Y, Chua S Jr. Leptin function and regulation. Compr Physiol 2017;8:351–69.

SUPPLEMENTARY MATERIALS AND METHODS

Immunofluorescence

Inguinal subcutaneous fat sections (4 μm) were stained with primary antibodies: leptin, TMEM26 (Abcam, Cambridge, United Kingdom), or ZIC1 (Invitrogen, Carlsbad, CA) rabbit polyclonal antibodies, in a humidified chamber at 4 °C overnight. After washing with PBS, the sections were incubated with a secondary Alexa 488–conjugated goat anti-rabbit IgG (Invitrogen) antibody for 1 hour at room temperature. Nuclei were counterstained with DAPI for 10 minutes. The staining results are presented as images obtained using a confocal microscope (LSM 980 with Airyscan 2, Zeiss, Oberkochen, Germany).

Cell culture

Primary human dermal fibroblasts and primary human epidermal keratinocytes were isolated from foreskin. Human preadipocytes were isolated from subcutaneous adipose tissue obtained through elective liposuction. The collection and use of primary cells were approved by the Institutional Review Board at Seoul National University Hospital and conducted in accordance with the principles of the Declaration of Helsinki. All subjects provided written informed consent. Human epidermal keratinocytes were cultured in EpiLife medium containing human keratinocyte growth supplement (Thermo Fisher Scientific) in a 37 °C humidified, 5% carbon dioxide incubator. Human dermal fibroblasts and subcutaneous adipocytes were cultured in DMEM (Welgene, Daegu, Korea) containing 10% fetal bovine serum (Welgene) and penicillin/streptomycin (400 U/ml, 50 μg/ml). Human dermal fibroblasts and epidermal keratinocytes were seeded in culture dishes and, upon reaching confluence, were washed with PBS and irradiated with UV (100 mJ/cm^2) in PBS. Human preadipocytes were seeded in culture dishes and, upon reaching confluence, differentiated into adipocytes (Kim et al, 2011). Cells were washed with PBS and irradiated with UV (100 mJ/cm^2) in PBS. After UV irradiation, cells were maintained in DMEM medium without fetal bovine serum or EpiLife medium without growth supplement and harvested 24 hours after irradiation.

SUPPLEMENTARY REFERENCE

Kim EJ, Kim YK, Kim JE, Kim S, Kim MK, Park CH, et al. UV modulation of subcutaneous fat metabolism. J Invest Dermatol 2011;131:1720–6.

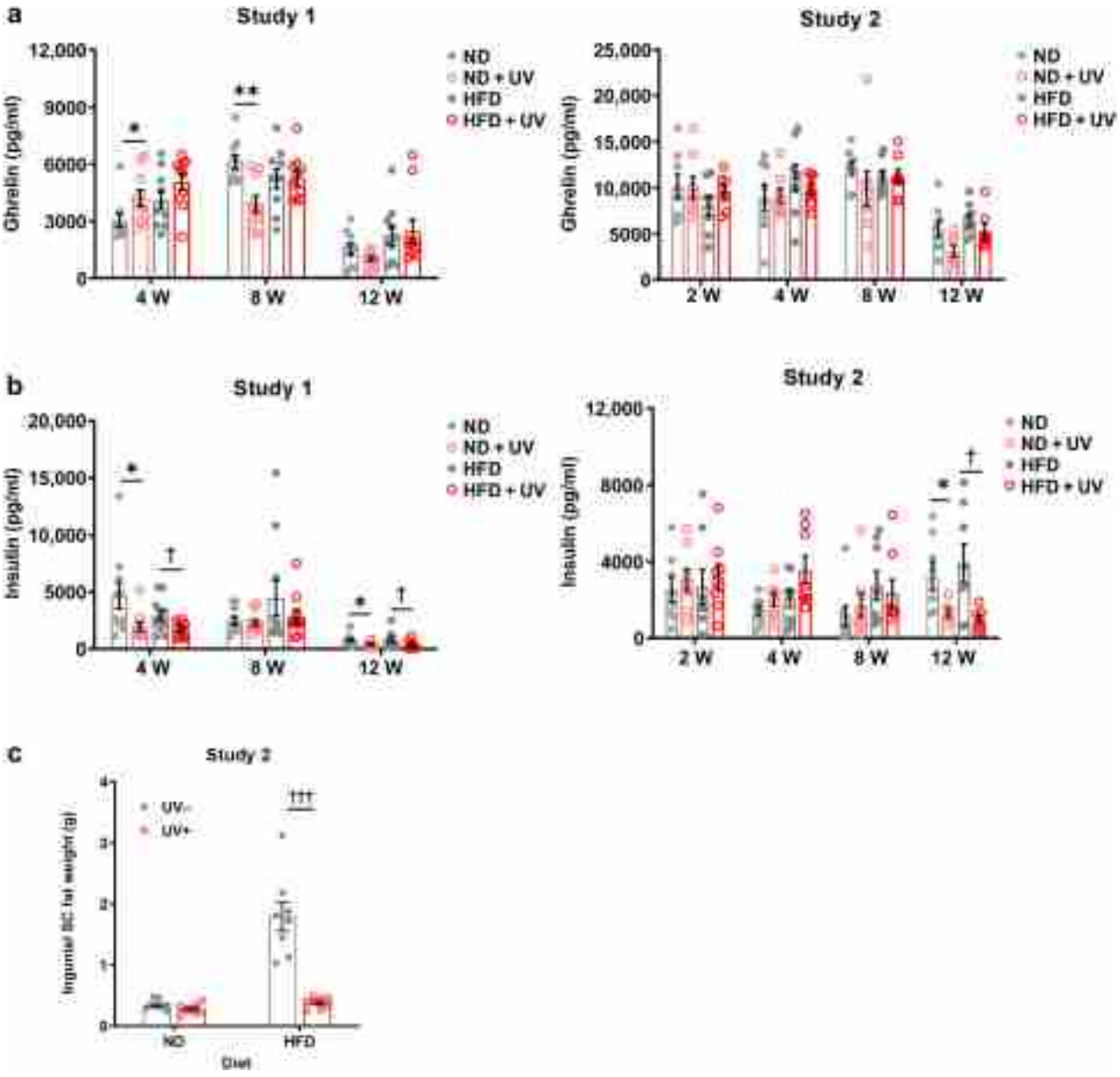

Supplementary Figure S1. Effect of UV irradiation on orexigenic and anorexigenic factors in mice. Serum samples were collected 24 h after the last UV irradiation at each indicated time point, after 6 h of fasting. **(a, b)** Serum ghrelin and insulin levels were measured using ELISA (study 1, n = 10 per group; study 2, n = 7−8 per group). **(c)** Inguinal fat tissues were weighed in study 2 after 12 weeks of UV irradiation (n = 7−8 per group). Data are presented as mean ± SEM. $^{*}P < .05$ and $^{**}P < .01$, the sham-irradiated ND-fed group versus the UV-irradiated ND-fed group; $^{\dagger}P < .05$ and $^{\dagger\dagger\dagger}P < .001$, the sham-irradiated HFD-fed group versus the UV-irradiated HFD-fed group. h, hour; HFD, high-fat diet; ND, normal diet; w, week.

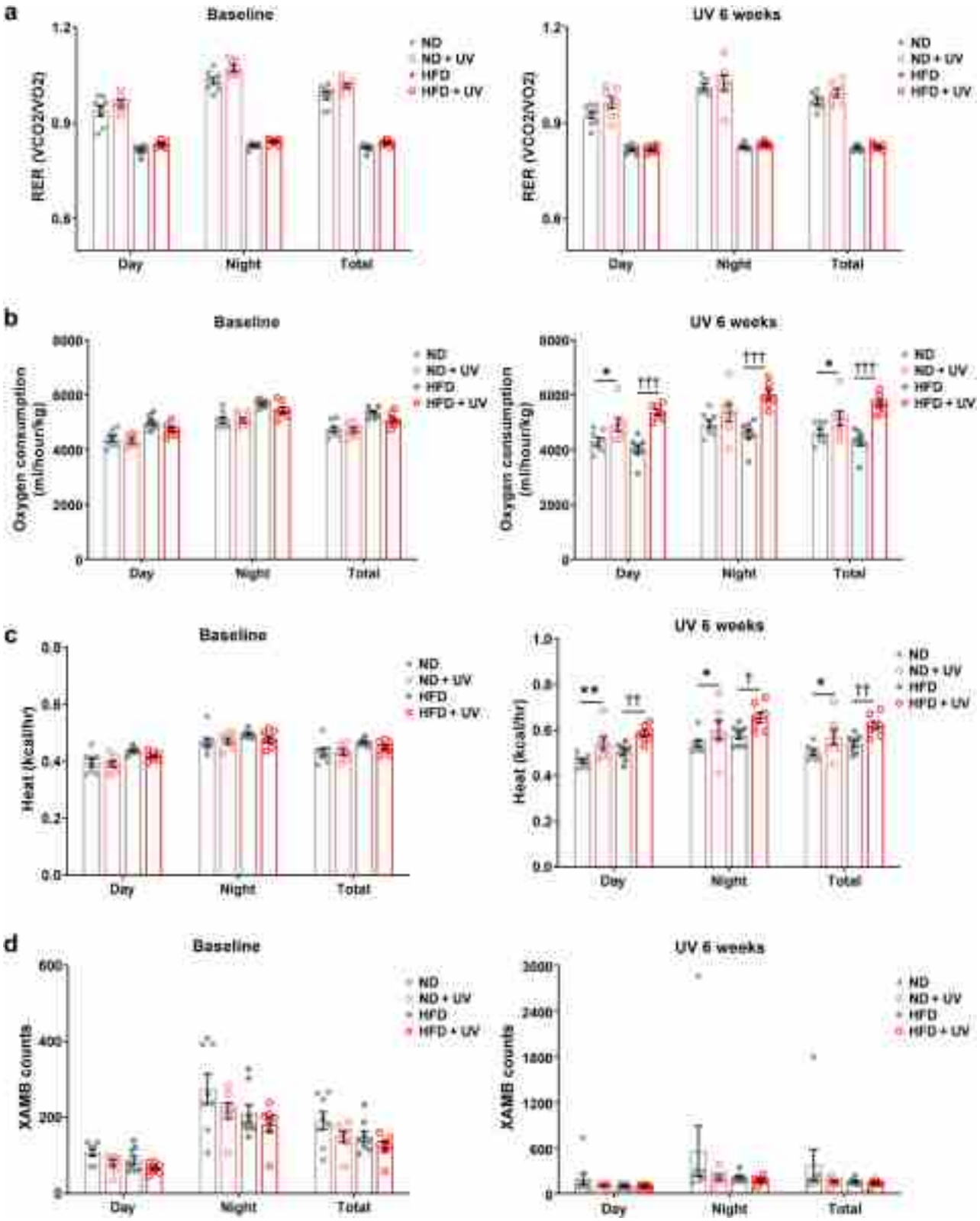

Supplementary Figure S2. Energy consumption increased in mice after 6 weeks of UV irradiation. The mice were kept alone in CLAMS cages at baseline and 6 weeks after UV irradiation. Data for **(a)** RER, **(b)** oxygen consumption, **(c)** heat generation, and **(d)** ambulatory activity counts (denoted as XAMB) during the light and dark cycles are shown. Data are presented as mean ± SEM (n = 7–8 per group). $^{*}P < .05$ and $^{**}P < .01$, the sham-irradiated ND-fed group versus the UV-irradiated ND-fed group; $^{\dagger}P < .05$, $^{\dagger\dagger}P < .01$, and $^{\dagger\dagger\dagger}P < .001$, the sham-irradiated HFD-fed group versus the UV-irradiated HFD-fed group. CLAMS, Comprehensive Lab Animal Monitoring System; HFD, high-fat diet; ND, normal diet; RER, respiratory exchange ratio.

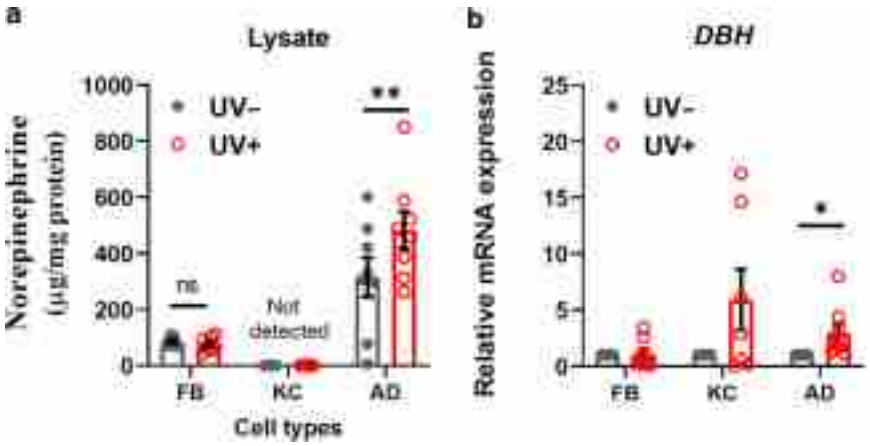

Supplementary Figure S3. Expression of NE levels in different types of primary cultured skin cells after 24 hours of UV irradiation. Primary human dermal FBs and primary human epidermal KCs were directly irradiated with UV (100 mJ/cm^2) upon reaching confluence. Human SC ADs were directly irradiated with UV (100 mJ/cm^2) after differentiation. **(a)** Dermal FBs (n = 7), epidermal KCs (n = 5), and ADs (n = 8) were harvested 24 hours after UV irradiation, and NE levels were measured in lysates of each cell type using an ELISA kit. **(b)** *DBH* mRNA expression levels were analyzed using quantitative PCR, with *36B4* serving as an endogenous control (n = 8). Data are presented as mean ± SEM. Significance was assessed using the paired *t*-test. $*P < .05$ and $**P < .01$, control group versus UV-irradiated group. AD, adipocyte; DBH, dopamine β-hydroxylase; FB, fibroblast; KC, keratinocyte; NE, norepinephrine; SC, subcutaneous.

Supplementary Table S1. Expression of 28 Neurotransmitters in Skin from UV-Irradiated Mice

		Concentration (ng/g Tissue)				Fold Change				*P*-Value	
	Neurotransmitter	ND	ND + UV	HFD	HFD + UV	ND	ND + UV	HFD	HFD + UV	ND Versus ND + UV	HFD Versus HFD + UV
1	**Norepinephrine**	15,642.0	22,622.7	37,262.7	75,454.9	1.0	1.4	2.4	4.8	[1]	[2]
2	GABA	322.3	1008.0	524.7	801.3	1.0	3.1	1.6	2.5	[3]	[2]
3	Aspartate	10,928.9	16,793.3	12,406.5	33,477.4	1.0	1.5	1.1	3.1	[1]	[4]
4	Glutamate	146,608.0	260,286.5	175,301.5	440,214.2	1.0	1.8	1.2	3.0	[1]	[4]
5	5-HT	124.5	490.5	19.7	737.9	1.0	3.9	0.2	5.9	[1]	[4]
6	DA	1642.1	2708.9	3704.1	4164.0	1.0	1.6	2.3	2.5	[1]	
7	Agmatine	12.5	38.2	22.7	33.0	1.0	3.1	1.8	2.6	[5]	
8	Glutamine	184,297.3	230,726.6	155,687.1	286,284.4	1.0	1.3	0.8	1.6		[4]
9	Choline	29,694.5	45,117.7	32,232.1	46,721.3	1.0	1.5	1.1	1.6		[2]
10	5-HIAA	331.8	589.1	279.0	1310.0	1.0	1.8	0.8	3.9		[4]
11	Ach	52.2	59.2	48.3	73.7	1.0	1.1	0.9	1.4		[6]
12	Dynorphin A	5.5	6.5	5.0	6.5	1.0	1.2	0.9	1.2		[2]
13	Epinephrine	262.5	194.1	229.3	525.9	1.0	0.7	0.9	2.0		[2]
14	Spermine	39,615.6	35,364.6	23,668.0	37,299.8	1.0	0.9	0.6	0.9		[6]
15	3-MT	3.7	3.3	4.8	10.9	1.0	0.9	1.3	2.9		[6]
16	Substance P	381.9	421.3	501.4	574.0	1.0	1.1	1.3	1.5		
17	2-PE	16.0	13.4	24.9	7.3	1.0	0.8	1.6	0.5		
18	Leu-enkephalin	29.5	31.7	25.2	25.6	1.0	1.1	0.9	0.9		
19	Met-enkephalin	11.2	11.2	8.4	9.0	1.0	1.0	0.7	0.8		
20	N-acetyl-Asp-Glu	4437.3	4711.2	2234.4	1785.7	1.0	1.1	0.5	0.4		
21	Putrescine	4494.8	10,074.0	6457.4	9885.4	1.0	2.2	1.4	2.2		
22	Spermidine	69,243.7	114,680.7	94,786.1	144,177.8	1.0	1.7	1.4	2.1		
23	DOPAC	—	—	—	—	—	—	—	—	—	—
24	HVA	—	—	—	—	—	—	—	—	—	—
25	MHPG-sulfate	—	—	—	—	—	—	—	—	—	—
26	Tyramine	—	—	—	—	—	—	—	—	—	—
27	Tryptamine	—	—	—	—	—	—	—	—	—	—
28	Octopamine	—	—	—	—	—	—	—	—	—	—

Abbreviations: 3-MT, 3-methoxytyramine; 5-HIAA, 5-hydroxyindoleacetic acid; 5-HT, 5-hydroxytryptamine; DA, dopamine; DOPAC, 3,4-dihydroxyphenylacetic acid; GABA, γ-aminobutyric acid; HFD, high-fat diet; HVA, homovanillic acid; MHPG, 3-methoxy-4-hydroxyphenylglycol; ND, normal diet; 2-PE, 2-phenylethanol.

The concentrations of 28 neurotransmitters were measured in the skin using liquid chromatography–tandem mass spectrometry. Data are represented as the mean (n = 7–8 mice per group) and were screened on the basis of fold change and statistical significance.

[1] $P < .05$ for the sham-irradiated ND-fed group versus the UV-irradiated ND-fed group.

[2] $P < .01$ for the sham-irradiated HFD-fed group versus the UV-irradiated HFD-fed group.

[3] $P < .01$ for the sham-irradiated ND-fed group versus the UV-irradiated ND-fed group.

[4] $P < .001$ for the sham-irradiated HFD-fed group versus the UV-irradiated HFD-fed group.

[5] $P < .001$ for the sham-irradiated ND-fed group versus the UV-irradiated ND-fed group.

[6] $P < .05$ for the sham-irradiated HFD-fed group versus the UV-irradiated HFD-fed group.

Supplementary Table S2. Primer Sequences Used in this Study

Gene	Forward	Reverse	Size (bp)
Mouse *Npy*	GTGTTTGGGCATTCTG	TTCTGTGCTTTCCTTCAT	193
Mouse *Agrp*	CTCGTTCTCCGCGTCGCTGTG	ACCCAGCTTGCGGCAGTAGCA	128
Mouse *Pomc*	CTGGAGCAACCCGCCCAAGGA	GCGCGTTCTTGATGATGGCGTTCT	107
Mouse *Cart*	GCCAAGTCCCCATGTGTGAC	CACCCCTTCACAAGCACTTCA	129
Mouse leptin	TCTCCGAGACCTCCTCCATCT	TTCCAGGACGCCATCCAG	100
Mouse *36b4*	TGCCACACTCCATCATCAAT	CGAAGAGACCGAATCCCATA	240
Human *DBH*	TCCCCTATCACATCCCCCTG	AGGAGCTGGAAATGGATGGC	91
Human *36B4*	TGGGCTCCAAGCAGATGC	GGCTTCGCTGGCTCCCAC	420

Abbreviations: Agrp, agouti-related protein; Cart, cocaine-and-amphetamine-responsive transcript; DBH, dopamine β-hydroxylase; Npy, neuropeptide Y; Pomc, pro-opiomelanocortin.